

ER $\alpha$  protein may be an obligatory step for acquisition of estrogen-ablation resistance.

Previously, the expression level of ER $\alpha$  transcript from promoter A was reported to be several folds higher than that from promoter C in MCF-7 cells [24,25], in good agreement with our current study for wild-type MCF-7 cells (Fig. 2). On the other hand, in this study, we for the first time demonstrated that ER $\alpha$  transcripts from promoters A and C expressed at high levels in LTED cells as compared with wild-type cells using real-time PCR (Fig. 2). Specifically, transcripts from promoter C in LTED cells were 149-fold higher than those in wild-type cells and the transcripts from promoter A and C were equally expressed in LTED cells (Fig. 2), indicating that enhanced transcription of ER $\alpha$  gene from promoter C may in part be responsible for the enhanced expression of ER $\alpha$  protein in LTED cells.

Our transient transfection experiments indicated that alterations of transcription factors may not be a major cause for the enhanced expression of ER $\alpha$  mRNA from promoter C in LTED cells (Fig. 3). On the other hand, methylation status of the promoter C region of ER $\alpha$  gene was drastically changed in LTED cells as compared with wild-type cells (Figs. 4–7). We have previously reported that specific *in vitro* methylation of promoter C region of ER $\alpha$  gene significantly reduced its promoter activity in transient transfection experiment [20]. In addition, methylation of promoter C was inversely associated with expression of transcripts from this promoter as well as ER $\alpha$  protein in primary breast cancer [20]. Taken together, hypomethylation of promoter C region in LTED cells can be one of the mechanisms responsible for the enhanced transcription of ER $\alpha$  gene from promoter C.

In this study, we demonstrated that ER $\alpha$  transcript from promoter A also expressed at high levels in LTED cells as compared with wild-type cells (Fig. 2). Since the promoter A was highly unmethylated in both LTED and wild-type MCF-7 cells (Fig. 4), some mechanisms other than DNA methylation should be involved in the regulation of promoter A in LTED cells. Our transient transfection experiments did not show any difference of the reporter gene activity of promoter A constructs in between LTED and wild-type MCF-7 cells (Fig. 3). One possible explanation for the enhanced expression of the transcript from promoter A in LTED cells could be alteration of transcription factors that bind to downstream sequences including intron of the ER $\alpha$  gene that are not present in our tested construct; AP2 transcription factor that bind to the ERF-1 *cis*-acting element located downstream of the transcription start site of promoter A may be one of the candidates [18,19].

Transcripts from promoter A and C share an identical coding sequence for ER $\alpha$  protein. Then, is there any functional difference between these transcripts in relation to the protein level of ER $\alpha$ ? Importantly, it has recently been shown that 5' upstream open reading frame (ORF) that is specific to the transcript A has inhibitory effects on the translation of ER $\alpha$  protein, while the 5' upstream ORF of transcript C did not show the effect [26]. Notably, the inhibitory effect of the ORF

of transcript A was most remarkable in MCF-7 cells among the tested cell lines, indicating that there are differences in the translational potential of transcripts from these two major promoters [26]. It would be interesting to test whether such regulatory effects of upstream ORF specific to transcript A is also present in MCF-7 LTED cells.

In conclusion, we found that transcription from promoters A and C were highly activated in LTED cells. Specifically, hypomethylation of promoter C correlated well with its drastically enhanced expression in LTED cells, suggesting that epigenetic alterations may play some roles in enhanced expression of ER $\alpha$  important for the acquisition of estrogen-ablation resistance of breast cancer cells.

### Acknowledgements

We thank Ms. Shoko Hirano for her excellent technical assistance. This work was supported in part by a Grant-in-Aid for Science, Ministry of Education, Culture, Sports, Science, and Technology, Japan.

### References

- [1] V.C. Jordan, Selective estrogen receptor modulation: concept and consequences in cancer, *Cancer Cell* 5 (3) (2004) 207–213.
- [2] W. Yue, J.P. Wang, Y. Li, W.P. Bocchinfuso, K.S. Korach, P.D. Devanean, E. Rogan, E. Cavalieri, R.J. Santen, Tamoxifen versus aromatase inhibitors for breast cancer prevention, *Clin. Cancer Res.* 11 (2) (2005) 925–930.
- [3] R.J. Santen, H.A. Harvey, Use of aromatase inhibitors in breast carcinoma, *Endocr. Relat. Cancer* 6 (1) (1999) 75–92.
- [4] R.J. Santen, A. Manni, H.A. Harvey, C. Redmond, Endocrine treatment of breast cancer in woman, *Endocr. Rev.* 11 (2) (1990) 221–265.
- [5] S. Masamura, S.J. Santner, D.F. Heitjan, R.J. Santen, Estrogen deprivation causes estradiol hypersensitivity in human breast cancer cells, *J. Clin. Endocrinol. Metab.* 80 (10) (1995) 2918–2925.
- [6] M.H. Jeng, M.A. Shupnik, T.P. Bender, E.H. Westin, D. Bandyopadhyay, R. Kumar, S. Masamura, R.J. Santen, Estrogen receptor expression and function in long-term estrogen-deprived human breast cancer cells, *Endocrinology* 139 (10) (1998) 4164–4174.
- [7] R.X. Song, R.A. McPherson, L. Adam, Y. Bao, M. Shupnik, R. Kumar, R.J. Santen, Linkage of rapid estrogen action to MAPK activation by ER $\alpha$ -Shc association and Shc pathway activation, *Mol. Endocrinol.* 16 (1) (2002) 116–127.
- [8] D. Zivadinovic, C.S. Watson, Membrane estrogen receptor- $\alpha$  levels predict estrogen-induced ERK1/2 activation in MCF-7 cells, *Breast Cancer Res.* 7 (1) (2005) 130–144.
- [9] W. Yue, J.P. Wang, M. Conaway, S. Masamura, Y. Li, R.J. Santen, Activation of the MAPK pathway enhances sensitivity of MCF-7 breast cancer cells to the mitogenic effort of estradiol, *Endocrinology* 143 (9) (2002) 3221–3229.
- [10] Z. Zhang, R. Kumar, R.J. Santen, R.X. Song, The role of adapter protein Shc in estrogen non-genomic action, *Steroids* 69 (8/9) (2004) 523–529.
- [11] R.J. Santen, R.X. Song, Z. Zhang, R. Kumar, M.H. Jeng, S. Masamura, J. Lawrence, L. Berstein, W. Yue, Long-term estradiol deprivation in breast cancer cells up-regulates growth factor signaling and enhances estrogen sensitivity, *Endocr. Relat. Cancer* 12 (Suppl. 1) (2005) 61–73.
- [12] M. Koš, G. Reid, S. Denger, F. Gannon, Minireview: genomic organization of the human ER $\alpha$  gene promoter region, *Mol. Endocrinol.* 15 (12) (2001) 2057–2063.

- [13] G. Flouriot, C. Griffin, M. Kenealy, V. Sonntag-Buck, F. Gannon, Differentially expressed messenger RNA isoforms of the human estrogen receptor- $\alpha$  gene are generated by alternative splicing and promoter usage, *Mol. Endocrinol.* 12 (12) (1998) 1939–1954.
- [14] A. Malyala, M.J. Kelly, O.K. Rønnekleiv, Estrogen modulation of hypothalamic neurons: activation of multiple signaling pathways and gene expression changes, *Steroids* 70 (5–7) (2005) 397–406.
- [15] K.M. Österlund, K. Grandied, E. Keller, Y.L. Hurd, The human brain has distinct regional expression patterns of estrogen receptor  $\alpha$  mRNA isoforms derived from alternative promoters, *J. Neurochem.* 75 (4) (2000) 1390–1397.
- [16] S. Hayashi, K. Imai, K. Suga, T. Kurihara, Y. Higashi, K. Nakachi, Two promoters in expression of estrogen receptor messenger RNA in human breast cancer, *Carcinogenesis* 18 (3) (1997) 459–464.
- [17] K. Tanimoto, H. Eguchi, T. Yoshida, K. Hajiro-Nakanishi, S. Hayashi, Regulation of estrogen receptor  $\alpha$  gene mediated by promoter B responsible for its enhanced expression in human breast cancer, *Nucl. Acids Res.* 27 (3) (1999) 903–909.
- [18] E.C. deConinck, L.A. McPherson, R.J. Weigel, Transcriptional regulation of estrogen receptor in breast carcinomas, *Mol. Cell. Biol.* 15 (4) (1995) 2191–2196.
- [19] L.A. McPherson, V.R. Baichwal, R.J. Weigel, Identification of ERF-1 as a member of the AP2 transcription factor family, *Proc. Natl. Acad. Sci. U.S.A.* 94 (9) (1997) 4342–4347.
- [20] T. Yoshida, H. Eguchi, K. Nakachi, K. Tanimoto, Y. Higashi, K. Suemasu, Y. Iino, Y. Morishita, S. Hayashi, Distinct mechanisms of loss of estrogen receptor  $\alpha$  gene expression in human breast cancer: methylation of the gene and alteration of *trans*-acting factor, *Carcinogenesis* 21 (12) (2000) 2193–2201.
- [21] N. Yoshida, Y. Omoto, A. Inoue, H. Eguchi, Y. Kobayashi, M. Kurosumi, S. Saji, K. Suemasu, T. Okazaki, K. Nakachi, T. Fujita, S. Hayashi, Prediction of prognosis of estrogen receptor-positive breast cancer with combination of selective estrogen-regulated genes, *Cancer Sci.* 95 (6) (2004) 496–502.
- [22] G.J. Herman, R.J. Graff, S. Myöhänen, D.B. Nelkin, B.S. Baylim, Methylation-specific, PCR: a novel PCR assay for methylation status of CpG islands, *Proc. Natl. Acad. Sci. U.S.A.* 93 (18) (1996) 9821–9826.
- [23] L.C. Li, R. Dahiya, MethPrimer: designing primers for methylation PCRs, *Bioinformatics* 18 (11) (2002) 1427–1431.
- [24] M.J. Fasco, Estrogen receptor mRNA splice variants produced from the distal and proximal promoter transcripts, *Mol. Cell. Endocrinol.* 138 (1998) 51–59.
- [25] R.J. Weigel, D.L. Crooks, J.D. Iglehart, E.C. deConinck, Quantitative analysis of the transcriptional start sites of estrogen receptors in breast carcinoma, *Cell Growth Differ.* 6 (1995) 707–711.
- [26] B.T. Pentecost, R. Song, M. Luo, J.A. DePasquale, M.J. Fasco, Upstream regions of the estrogen receptor alpha proximal promoter transcript regulate ER protein expression through a translational mechanism, *Mol. Cell Endocrinol.* 229 (2005) 83–94.

## Mutation profile of *EGFR* gene detected by denaturing high-performance liquid chromatography in Japanese lung cancer patients

Naoko Sueoka · Akemi Sato · Hidetaka Eguchi · Kazutoshi Komiya · Toru Sakuragi · Masahiro Mitsuoka · Toshimi Satoh · Shinichiro Hayashi · Kei Nakachi · Eisaburo Sueoka

Received: 15 May 2006 / Accepted: 30 June 2006 / Published online: 1 September 2006  
© Springer-Verlag 2006

### Abstract

**Purpose** *EGFR* mutations in lung cancer increase sensitivity to an *EGFR* tyrosine kinase inhibitor, gefitinib. Mutation analysis of *EGFR* is essential for prediction of gefitinib response and avoidance of the coincidental severe side effects for the unresponsive population. The purpose of the present study is to apply DHPLC as a screening system of detection of *EGFR* mutations for large scaled population.

**Methods** *EGFR* mutations were detected by both DHPLC procedure and direct sequencing using lung cancer tissue samples obtained from 97 patients (81 surgical specimens and 16 pleural effusions of non-resectable lung cancer patients).

**Results** DHPLC analysis detected *EGFR* mutations in 5 h as opposed to 18 h by direct sequencing for ten samples, and it costs eightfold more expensive by direct sequencing than DHPLC. In addition, DHPLC analysis was sixfold more sensitive than sequencing

analysis for detection of the point mutation of exon 21, L858R. Using this system, *EGFR* mutations in exons 18, 19 and 21 were found in 34 of 97 patients (36%). Thirteen of the 15 patients with exon 21 mutations (87%) were female non-smokers, who were diagnosed with adenocarcinomas with the feature of BAC. Eight of the 18 patients with exon 19 mutations (44%) were 7 male and 1 female current or former smokers, and BAC feature was observed in 61% (8/18).

**Conclusion** DHPLC analysis for screening followed by sequencing analysis appears to be more sensitive and accurate, as well as easier and faster. In addition, these results suggest different mutagenesis and carcinogenesis pathways for mutations.

**Keywords** Lung cancer · *EGFR* mutation · DHPLC · BAC

### Abbreviations

AAH	Atypical adenomatous hyperplasia
BAC	Bronchioloalveolar carcinoma
CT	Computed tomography
DHPLC	Denaturing high-performance liquid chromatography
EGFR	Epidermal growth factor receptor
TEAA	Triethylammonium acetate

### Introduction

Lung cancer is the most common cause of cancer death among males in Japan, accounting for 23.1% of all male cancer deaths, and it ranks third among females (12.6%) ("Cancer Statistics in Japan" Editorial Board 2005). Despite significant progress in the treatment of lung

N. Sueoka (✉) · A. Sato · K. Komiya · S. Hayashi · E. Sueoka  
Department of Internal Medicine, Faculty of Medicine,  
Saga University, 5-1-1 Nabeshima, Saga, 849-8501, Japan  
e-mail: sueokan@cc.saga-u.ac.jp

H. Eguchi · K. Nakachi  
Department of Radiobiology and Molecular  
Epidemiology, Radiation Effects Research Foundation,  
Hiroshima, Japan

T. Sakuragi · M. Mitsuoka  
Department of Thoracic Surgery, Faculty of Medicine,  
Saga University, Saga, Japan

T. Satoh  
Department of Pathology, Faculty of Medicine,  
Saga University, Saga, Japan

cancer, its overall prognosis is poor: a 5-year survival rate of 14%, and especially poor prognosis for non-resectable advanced cases (Mountain and Dresler 1997). Among new therapeutic strategies, a quinazoline-derived EGFR tyrosine kinase inhibitor, gefitinib, showed profound response in a subgroup of non-small cell lung cancer, most of whom were female non-smokers with adenocarcinomas (Lynch et al. 2004; Kim and Choy 2004).

EGFR, a member of the ErbB family for receptor tyrosine kinases, is a 170 kDa transmembrane glycoprotein which contains an extracellular ligand-binding region, a hydrophobic transmembrane domain, a tyrosine kinase domain and a carboxyl autophosphorylation region. Normally, ligand binding to EGFR causes receptor dimerization and tyrosine kinase activation, resulting in regulation of cell proliferation through the RAS/MAPK pathway, and cell survival and transformation through the PI3K/AKT pathway (Jorissen et al. 2003). Recently, somatic mutations of *EGFR* in lung cancer tissues were observed: The mutations enhanced its tyrosine kinase activity and increase the sensitivity of the tumor to gefitinib, an EGFR-tyrosine kinase inhibitor (Lynch et al. 2004; Paez et al. 2004). These mutant EGFRs selectively activated the AKT and STAT signaling pathways, which contribute to cell survival (Sordella et al. 2004). Various mutations in exons 18 and 21 have subsequently been reported, and these mutations are clustered near the ATP cleft of the tyrosine kinase domain (Pao et al. 2004; Kosaka et al. 2004; Tokumo et al. 2005; Yang et al. 2005). Functional analysis of the mutations showed stabilization in their interaction with both ATP and gefitinib based on evidence of increased receptor activation after ligand binding and enhanced inhibition induced by gefitinib (Lynch et al. 2004). In fact, the response rates of gefitinib among patients with *EGFR* mutations were high: 65% (11/17) in Korea and 89% (8/9) in Japan (Tokumo et al. 2005; Han et al. 2005). The frequency of *EGFR* mutations among gefitinib or erlotinib responsive patients was 71% (12/17) in USA, and 78% (7/9) in Taiwan (Pao et al. 2004; Huang et al. 2004). Detailed DNA sequence analysis has recently revealed a second point mutation, T790M, using a tumor biopsy specimen obtained at the time of relapse (Kobayashi et al. 2005). In contrast to the response of gefitinib, severe adverse effects, such as acute lung injury, have also been reported (AstraZeneca 2004, in-house data). A multicenter prospective review in Japan showed that gefitinib-induced interstitial lung disease occurred in 215 of the 3,222 cases (5.8%), of which 83 (2.6%) died. Therefore, it is clear that the DNA sequence analysis of *EGFR* in lung cancer is essential for prediction of gefitinib response.

Direct sequencing approach for detection of *EGFR* mutations, which is a standard method, is not easy and is time-consuming. To seek easier and more sensitive approach, we applied Denaturing high-performance liquid chromatography (DHPLC) and compared the sensitivity, cost-effectiveness and analysis time with direct sequencing method. In this paper, we show that analysis time by DHPLC was one-fourth of that by direct sequencing, and running cost was low. In addition, DHPLC analysis was sixfold more sensitive than sequencing analysis for detection of the point mutation of exon 21, L858R. Thus, DHPLC followed by direct sequencing for detection of mutation type is more accurate and cost-effective. Using this approach, we investigated the clinicopathological relationship of *EGFR* mutations and showed the different characteristics between exons 19 and 21 mutations among Japanese lung cancer patients. Considering these evidences, dependable method for detection of *EGFR* mutations is urgently needed for not only prediction of response to gefitinib, but also detailed analysis of lung carcinogenesis associated with *EGFR* mutations. In this paper, we show the clinical application of DHPLC as a highly sensitive and useful screening system for detection of *EGFR* mutations in lung cancer tissues.

## Materials and methods

### Tissue samples, pleural effusion

Tissue samples were obtained from 81 surgical specimens of lung cancer patients, and pleural effusions were obtained from 16 non-resectable lung cancer patients. Study patients had been admitted to Saga Medical School Hospital between 2000 and 2005, and had not received any anticancer chemotherapy or thoracic irradiation. Clinical stage was determined by the criteria of the International Union Against Cancer, and informed consent was obtained from all subjects. Histological subtype and tumor content were confirmed by HE staining using adjacent tumor samples. Pleural effusion used for analysis was assessed as class V by pathologist. A total of 97 study patients were investigated on *EGFR* mutation status by both DNA direct sequencing and DHPLC.

### DNA extraction and sequencing analysis

DNA was isolated from fresh frozen tissues from tumors using QIAamp® DNA mini kit (QIAGEN, Hilden, Germany) as manufacturer's instructions. The mutations of exons 18, 19 and 21 were determined by

PCR-based direct sequencing. The primers for *EGFR* previously described were used. PCR amplification was performed in 20- $\mu$ l volume using Discoverase<sup>TM</sup> DHPLC DNA polymerase (Invitrogen Inc., CA) at 95°C for 10 min, then 40 cycles at 95°C for 30 s, 58°C for 30 s, 72°C for 1 min and a final extension at 72°C for 10 min. The amplified product was isolated using Microcon YM-50 (Millipore Inc. MA), and sequenced directly using Applied Biosystems PRISM dye terminator cycle sequencing method with ABI PRISM 3100 Genetic Analyzer (Applied Biosystems, Foster City, CA).

#### Denaturing high-performance liquid chromatography

PCR amplification was performed as described above. The primer sets used for DHPLC were as follows: sense: 5'-CAACCAAGCTCTCTTGAGGATC-3' and antisense: 5'-CCCAGCCCAGAGGCCTGT-3' (amplicon size, 115 bp) for exon 18; sense: 5'-GCAGCATGTGGCACCATCTC-3' and antisense: 5'-AGAGCCATGGACCCCCACAC-3' (amplicon size, 197 bp) for exon 19; sense: 5'-TCTGTCCCTCACAGCAGGGTCT-3' and antisense: 5'-GCTGGCTGACCTAAAGCCAC-3' (amplicon size, 218 bp) for exon 21. Amplification was confirmed by agarose gel electrophoresis of PCR products followed by staining with ethidiumbromide. The PCR products were denatured at 94°C for 4 min and gradually cooled to 25°C for a heteroduplex formation. Unpurified PCR samples were separated on a heated C18 reverse phase column using 0.1 M TEAA in water and 0.1 M TEAA in 25% acetonitrile at a flow rate of 0.9 ml/min. Sample analysis temperatures were predicted using the WAVEMaker<sup>TM</sup> software (Transgenomic Inc., NE). Predicted melting temperatures for exons 18 and 21 were 61.4 and 61.2°C for heteroduplex separation, respectively. The analysis for exon 19 was undergone by size-dependent separation at 50°C.

#### Statistical analysis

The association between *EGFR* mutations and clinicopathological parameters were examined by chi-square test for contingency tables.

## Results

One patient with exon 21 mutation detected only by DHPLC, but not by direct sequencing

Although the detection of *EGFR* mutations is pivotal for prediction of gefitinib response as well as investiga-

tion of the mechanisms of lung carcinogenesis, the sequencing analysis is not easy and time-consuming. To find an easier and faster method for detection of *EGFR* mutations, we performed DHPLC along with sequencing analysis for exons 18, 19 and 21 using 97 lung cancer patients. A total of 97 lung cancer patients, 14 squamous cell carcinomas, 76 adenocarcinomas and 7 others (6 large cell carcinomas and 1 carcinosarcoma), were studied. Representative results of direct sequencing and DHPLC with *EGFR* mutations are shown in Fig. 1 and 2. *EGFR* mutations in exons 18, 19 and 21 were detected in 34 of 97 lung cancer patients (36%) (Table 1). A mutation in exon 18 was observed in a patient, and mutations in exon 19 were observed in 18 patients (15 surgical specimens and 3 pleural effusions) by DHPLC. These results were consistent with those by sequencing analysis (Table 2). Mutations in exon 21 were found in 15 patients (14 surgical specimens and 1 pleural effusion): 14 patients showed the mutations by both sequencing and DHPLC analyses, whereas one patient showed a mutation only by DHPLC. To confirm this mutation, we conducted sequencing analysis using fractionated samples obtained from a retention time of 5–6 min by DHPLC (Fig. 3). A mutation of exon 21, L858R, was apparently observed by sequencing analysis using fractionated samples, although the mutation was not detected by sequencing analysis using non-fractionated samples. A chest computed tomography (CT) scan and pathological finding of the patient are shown in Fig. 4. CT scan of the chest showed 2 cm lung mass in diameter, and pathological type was adenocarcinoma with the feature of BAC. The tumor specimen obtained for *EGFR* mutation analysis contained papillary adenocarcinoma with central scar formation, and the number of lung cancer cells was less than 20% (Fig. 4b).

#### Clinicopathological comparison of *EGFR* mutations between exons 19 and 21

The clinicopathological characteristics of lung cancer patients with *EGFR* mutation are shown in Table 1. Clear associations of *EGFR* mutations with gender (female), smoking status (non-smoker) and pathological typing (adenocarcinoma) were observed. Looking at the pathological type of lung cancer, the frequency of *EGFR* mutations was 43% (33/76) for adenocarcinoma, whereas no *EGFR* mutations were observed in squamous cell carcinoma. A mutation of exon 19 was detected in one carcinosarcoma. The frequency of *EGFR* mutations in female adenocarcinoma patients was 66% (25/38), whereas that in male adenocarcinoma patients was 24% (9/38), suggesting that both

**Fig. 1** *EGFR* mutations of exons 18, 19 and 21 in lung cancer tissue. **a** Heterozygous missense mutation (underline) of exon 18 (G719S). **b** Heterozygous in-frame deletion in exon 19 involving 15 bp from codons 746–750. Heterozygous missense mutation (underline) of exon 21 [L858R (**c**) and L861Q (**d**)]

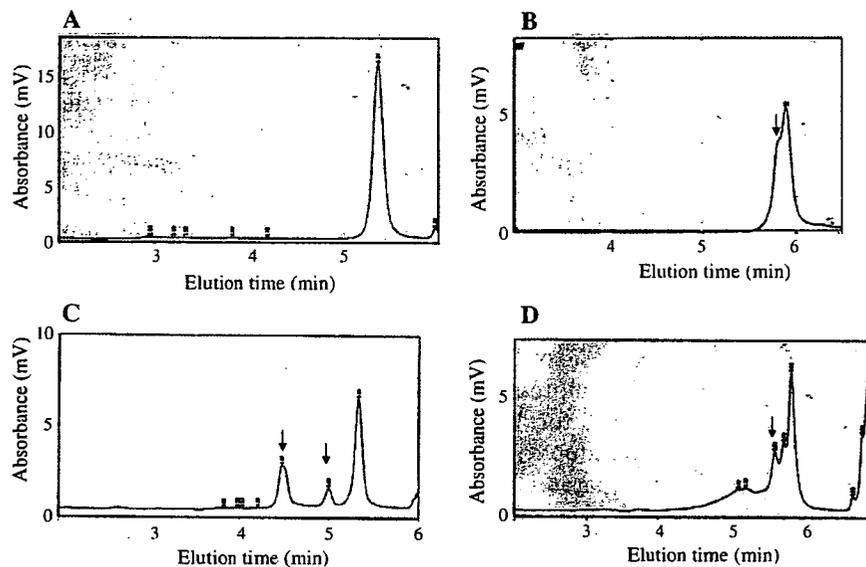
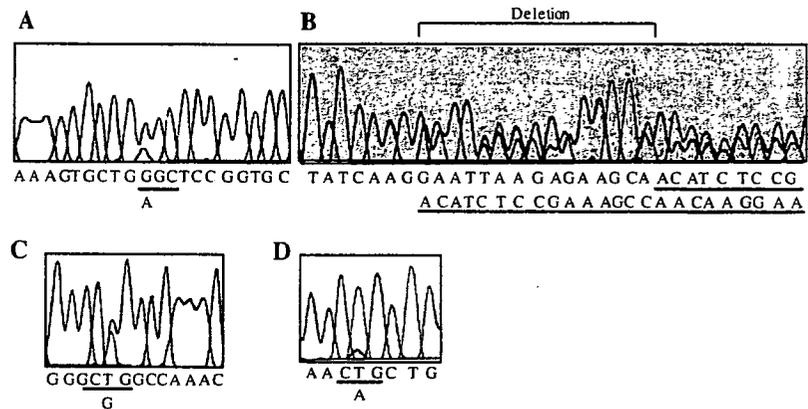


**Fig. 2** Detection of *EGFR* mutations using DHPLC. The mixture of PCR amplicons of wild type and mutant are denatured and re-annealed. Heteroduplexes and homoduplexes are isolated by different retention times in reverse-phase chromatography. Heteroduplexes are eluted earlier than homoduplexes, resulting in

detection of the mutations. Wild type of *EGFR* exon19 is shown in **a**. Mutations of exon 18, G719S (**b**), and 21, L858R (**d**), shows double-peak pattern (*arrows*). Mutation of exon 19, del E746-A750, was detected by size-dependent separation at 50°C, and short sized DNA fragments are eluted earlier (*arrows*) as shown in **c**

gender (female) and pathological type (adenocarcinoma) impacted *EGFR* mutations. One mutation in exon 18 and 15 mutations in exon 21 were point mutations (1 G719S, 14 L858R and 1 L861Q) (Table 4, Fig. 1), while 18 mutations in exon 19 were in-frame deletions of 9–24 bp around codons 746–759 (Table 3, Fig. 1). Thirteen of the 15 patients (87%) with exon 21 mutations were female non-smokers; the pathological types were all adenocarcinomas with features of BAC except for 2 patients (Table 4). A patient with exon 18 mutation was a female non-smoker with BAC. On the other hand, 8 of the 18 patients with exon 19 mutations were current or former smokers; 8 patients were men and lung cancer tissues of 7 did not reveal the feature of BAC (Table 3). The differences of pathological type,

including BAC or not, gender and smoking status between exons 21 and 19 were statistically significant (Table 5). These results suggest that different mechanisms of mutagenesis and carcinogenesis may exist between exons 19 and 21 mutations. Among these patients, seven patients, one with exon 21 mutation and six with exon 19 mutations, were treated with 250 mg gefitinib per day, and all patients responded, and gefitinib-induced lung injury was not observed.

#### Proposed screening system of *EGFR* mutations

To examine the sensitivity of DHPLC compared with sequencing analysis, we used H1975 cells with a point mutation of L858R. The point mutation was detected

**Table 1** Characteristics of patients with *EGFR* mutations

Age ± SD (yrs)		
With mutations		67.4 ± 11.1
Without mutations		67.5 ± 8.5
Sex		
Male		10/59 (17%)
Female		24/38 (63%)
		] P < 0.01
Smoking		
Smoker		10/57 (18%)
Non-smoker		24/40 (60%)
		] P < 0.01
Histology		
Squamous cell carcinoma		0/14 (0%)
Adenocarcinoma		33/76 (43%)
Others		1/7 (14%)
		] P < 0.01
Stage*		
I		24/58 (41%)
II		1/12 (8%)
III		6/14 (43%)
IV		3/13 (23%)
Total		34/97 (36%)

\*Postoperative pathological stage (clinical stage in 16 patients)

**Table 2** Comparison between DHPLC and sequence analysis on *EGFR* mutations

Exon 18			Exon 19			Exon 21		
Patient no.	DHPLC	Seq	Patient no.	DHPLC	Seq	Patient no.	DHPLC	Seq
1	M	M	1	M	M	1	M	M
			2	M	M	2	M	M
			3	M	M	3	M	M
			4	M	M	4	M	M
			5	M	M	5	M	M
			6	M	M	6	M	M
			7	M	M	7	M	M
			8	M	M	8	M	M
			9	M	M	9	M	M
			10	M	M	10	M	M
			11	M	M	11	M	M
			12	M	M	12	M	M
			13	M	M	13	M	M
			14	M	M	14	M	M
			15	M	M	15	M	M
			16	M	M			
			17	M	M			
			18	M	M			

Seq direct sequencing, M mutation

by direct-sequencing method when it contained more than 30% of H1975 cells, whereas the mutation was detected in the presence of, as little as, 5% of H1975 cells by DHPLC (Fig. 5). Comparison between DHPLC and direct sequencing in terms of analysis time for ten samples, *EGFR* mutations are detected in 5 h by DHPLC as opposed to 18 h by direct sequencing. In addition, it costs eightfold more expensive by direct sequencing than DHPLC. Thus, DHPLC is more sensitive, cost-effective and easier than direct

sequencing. Based on these evidences, we proposed the screening system shown in Fig. 6. *EGFR* mutations are screened by DHPLC, and subsequently direct sequencing is performed for confirmation of the mutations and analyses of the mutation types using only samples in which *EGFR* mutations are detected by DHPLC. This system enables us to provide quick results and DHPLC analysis using fractionated samples reveals more obvious results without subcloning technique.

**Fig. 3** Detection of *EGFR* mutation, L858R, using sequencing analysis of fractionated samples obtained by DHPLC system. Genomic DNA isolated from lung cancer tissue of patient no.3 with exon 21 mutation was conducted by DHPLC (a), followed by sequencing analysis using fractionated samples with retention time of 5–6 min. The results of sequencing analysis in the indicated period (asterisks) are shown in c–f, and a result of that using non-fractionated sample is shown in b

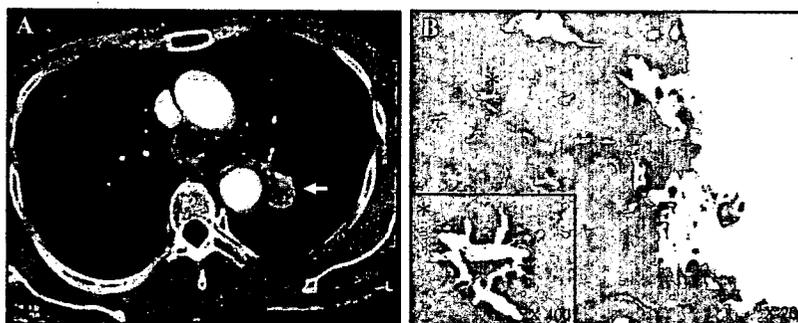
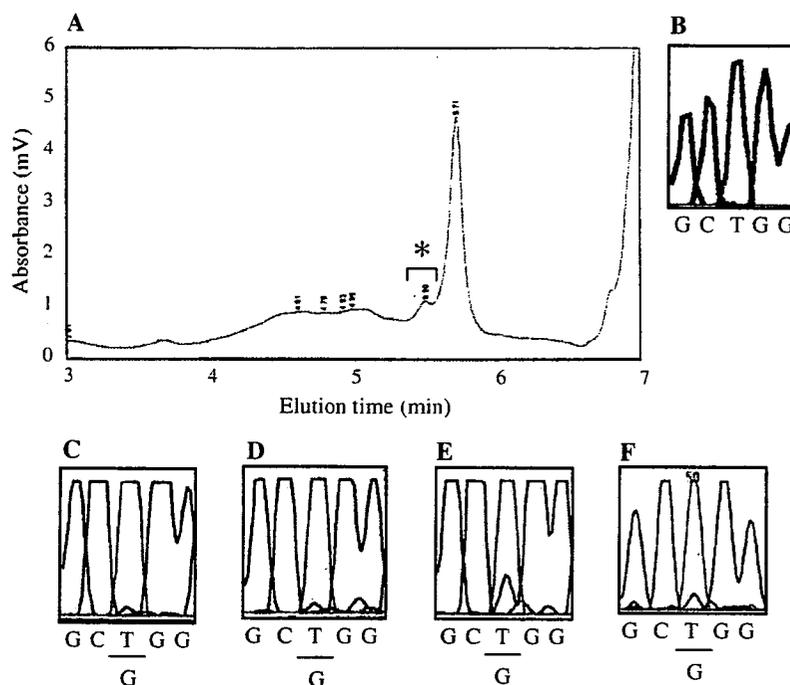


**Fig. 4** A case of lung cancer in which *EGFR* mutation of exon 21, L858R, was detected by only DHPLC and not direct sequencing. **a** CT scan of the chest showed 2 cm lung mass in left lung (white

arrow). **b** The tumor specimen obtained for mutation analysis, which contained papillary adenocarcinoma shown by 400-fold magnification (asterisks), with central scar formation

## Discussion

In this paper, we proposed new screening system for detection of *EGFR* mutations by DHPLC analysis. DHPLC analysis can detect mutations within 2–3 min by comparing two chromosomes as a mixture of denatured and reannealed PCR amplicons revealing discrete retention of homo- and heteroduplex DNA (Xiao and Oefner 2001). Since hot spots for mutations are present in the *EGFR* gene, which are associated with gefitinib response, DHPLC is a useful method for detection. In our study, results using DHPLC analysis were consistent with those of direct sequencing. In addition, DHPLC analysis was sixfold more sensitive than sequencing analysis for detection of the point

mutation of exon 21, L858R. It is difficult to detect the mutation by direct sequencing analysis using whole tissue samples when the number of lung cancer cells is low. Indeed, patient no. 3 with exon 21 mutation had a pure BAC pattern, and the number of lung cancer cells was low in tumor samples. The sequencing analysis did not detect a point mutation of exon 21, but DHPLC did. In addition to these benefits, DHPLC is cost-effective, which costs eightfold less expensive than direct sequencing. We therefore propose DHPLC for screening followed by sequencing as a more sensitive and accurate, as well as easier and faster, method.

Using this system, we also demonstrated differences in clinicopathological characteristics between the *EGFR* mutations of exons 19 and 21. Eighty seven per-



**Table 3** *EGFR* mutations of exon 19 in lung cancer tissues

No.	Sex	Mutation	Pathological type	BAC	Stage <sup>a</sup>	Smoking <sup>b</sup>	Gefitinib treatment
1	F	del L747-S752	ad	+	IA	0	Yes
2	M	del E746-A750	ad	–	IIIB	1,000	No
3	M	del L747-S752	ad	+	IIIB	50	No
4	F	del T751-E758	ad	+	IA	0	No
5	M	del E746-A750	ad	ND <sup>c</sup>	IIIB	15	Yes
6	M	del E746-A750	ad	–	IA	200	No
7	M	del E746-A750	Carcinosarcoma	–	IB	400	No
8	M	del L747-E749	ad	+	IA	200	No
9	F	del E746-A750	ad	+	IB	0	No
10	F	del L747-K754	ad	–	IB	0	No
11	F	del K745-E746	ad	ND	IV	300	Yes
12	M	del L747-T751	ad	ND	IV	760	Yes
13	F	del E746-A750	ad	+	IIIB	0	Yes
14	F	del E746-A750	ad	+	IA	0	No
15	F	del E746-A750	ad	+	IB	0	No
16	M	del E746-A750	ad	–	IA	0	No
17	F	del E746-A750	ad	–	IIIB	0	Yes
18	F	del E746-A750	ad	–	IIIB	0	No

M male, F female, ad adenocarcinoma, BAC bronchioalveolar carcinoma, ND not determined

<sup>a</sup> Postoperative pathological stage (clinical stage in patient no. 5, 11, 12)

<sup>b</sup> Smoking index: (number of cigarettes smoking/days) × years

<sup>c</sup> Diagnosis was made only from cytology of pleural effusion and biopsy specimen was not obtained

**Table 4** *EGFR* mutations of exon 21 in lung cancer tissues

No.	Sex	Mutation	Pathological type	BAC	Stage <sup>a</sup>	Smoking <sup>b</sup>	Treatment of gefitinib
1	F	L858R	ad	+	IA	0	No
2	F	L858R	ad	+	IA	0	No
3	F	L858R	ad	+	IA	0	No
4	F	L858R	ad	+	IA	0	No
5	F	L858R	ad	+	IA	0	No
6	F	L858R	ad	+	IA	0	Yes
7	F	L858R	ad	+	IA	0	No
8	F	L858R	ad	+	IA	0	No
9	F	L858R	ad	ND <sup>c</sup>	IV	0	No
10	F	L861Q	ad	+	IA	0	No
11	M	L858R	ad	–	IB	1,000	No
12	F	L858R	ad	+	IA	0	No
13	F	L858R	ad	+	IIIB	0	No
14	M	L858R	ad	+	IA	200	No
15	F	L858R	ad	+	IA	0	No

M male, F female, ad adenocarcinoma, BAC bronchioalveolar carcinoma, ND not determined

<sup>a</sup> Postoperative pathological stage (clinical stage in patient no. 9)

<sup>b</sup> Smoking index: (number of cigarettes smoking/days) × years

<sup>c</sup> Diagnosis was made only from cytology of pleural effusion and biopsy specimen was not obtained

cent of the patients with exon 21 mutations were non-smokers and/or women, and their pathological types were adenocarcinoma with the feature of BAC. On the other hand, 44% of those with exon 19 mutations had a smoking history and included eight male patients, with BAC feature not observed in 39% of these patients. Another group also reported that gender difference was observed for mutational location dominance of

exon 19 for males and exon 21 for females among Japanese lung cancer patients (Tokumo et al. 2005). These results suggest discrete mechanisms of mutagenesis in *EGFR* gene and carcinogenesis pathway between exons 19 and 21.

*EGFR* mutations, including both exons 19 and 21, were recently reported to be observed even in histologically normal bronchial and bronchiolar epithelium of

**Table 5** Comparison between exons 19 and 21 mutations in lung cancer samples

	Female	Non-smoker	BAC*
Exon 21	13/15 (87%)	13/15 (87%)	13/14 <sup>‡</sup> (93%)
Exon 19	10/18 (56%)	10/18 (56%)	8/15 <sup>‡</sup> (53%)

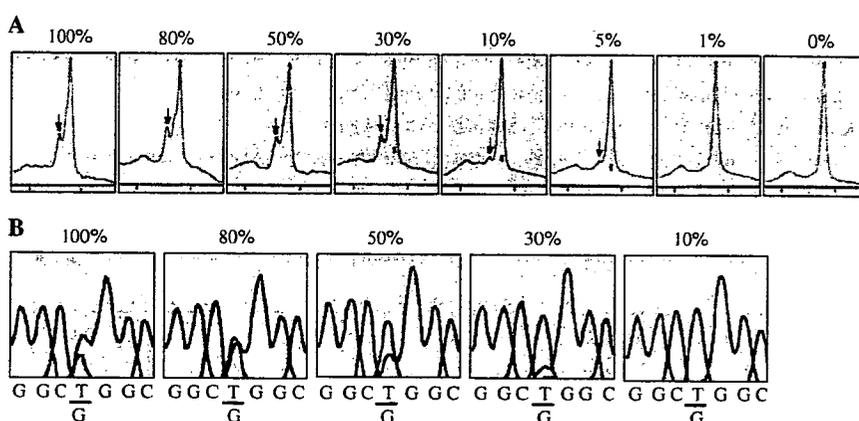
$p=0.05$  (between Female and Non-smoker for both exons)  
 $p=0.05$  (between Non-smoker and BAC\* for both exons)  
 $p=0.02$  (between Female and BAC\* for both exons)

BAC bronchioloalveolar carcinoma

\*Adenocarcinoma with BAC

<sup>‡</sup>The cases whose diagnosis was made only from cytology of pleural effusion were excluded

**Fig. 5** Comparison of the sensitivity to *EGFR* mutation in exon 21 between DHPLC (a) and sequencing analysis (b). H1975 cells, which have a point mutation of L858R, were used for the comparison. The indicated ratio of mixture with A549 cells, which do not have the mutation, was conducted with DHPLC or sequencing analysis



lung cancer patients with *EGFR* mutations in tumor cells (Tang et al. 2005), suggesting that both *EGFR* mutations are early events of lung carcinogenesis. However, it is possible that the factors inducing *EGFR* mutations are different, depending on the mutation types. It has also been reported that the patterns of *TP53* mutations depend on smoking status: G:C-to-T:A transversions and A:T-to-G:C transitions were consistently associated with smoking, whereas G:C-to-A:T transitions were associated with never-smokers, who had been highly exposed to occupational and environmental lung mutagenesis (Le Calvez et al. 2005). *KRAS* mutations are also frequently observed in adenocarcinoma, even in atypical adenomatous hyperplasia (AAH), which is the premalignant lesion of adenocarcinoma (Le Calvez et al. 2005; Westra et al. 1996). However, these mutations were associated with former smoker (Le Calvez et al. 2005), and the populations with *KRAS* mutations and *EGFR* mutations were discrete (Kosaka et al. 2004). Considering these evidences, we assume that types of *EGFR* mutations could depend on the etiology; mutations in exon 19 are partly

related with smoking and those in exon 21 are related with the other factors. In addition, we found different pathological types carrying *EGFR* mutations: exon 21 mutations had adenocarcinoma with the feature of BAC, and exon 19 mutations had adenocarcinoma without BAC. Noguchi et al. (1995) subdivided small, early adenocarcinomas into two groups: replacing growth type and non-replacing type. Their concept was that peripheral adenocarcinoma of the lung undergoes sequential progression from AAH through localized BAC to advanced localized BAC with fibroblastic proliferation. The accumulation of multiple allelic losses was observed during the sequential progression of replacing growth type (Aoyagi et al. 2001), whereas the non-replacing type was thought to be de novo adenocarcinomas without stepwise progression (Noguchi et al. 1995). Recently, Yatabe et al. (2005) reported that *EGFR* mutations in exon 21 were observed in two cases of AAH. These results suggest that the process of lung carcinogenesis may be different between two groups of *EGFR* mutations, exons 19 and 21.

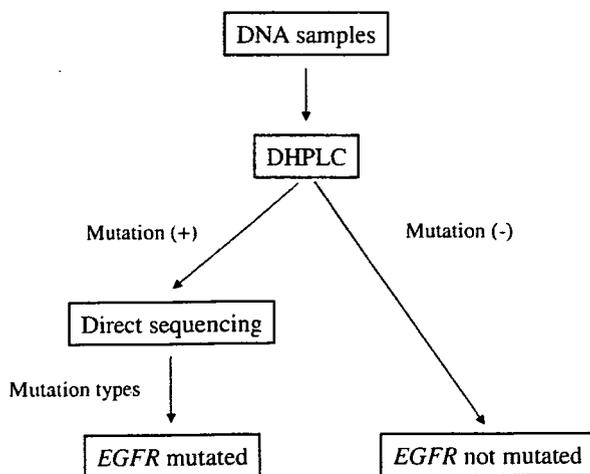


**Fig. 6** Proposed screening system of *EGFR* mutations. *EGFR* mutations are screened by DHPLC. When *EGFR* mutations are detected by DHPLC, direct sequencing is subsequently performed for confirmation of the mutations and analyses of the mutation types

We show in this paper that the response to gefitinib was observed in all patients with *EGFR* mutations, and the response rates of gefitinib among patients with *EGFR* mutations were from 80 to 90% in other reports (Tokumo et al. 2005; Han et al. 2005; Huang et al. 2004), suggesting the usefulness of detection of *EGFR* mutations for the prediction of gefitinib response. Analysis of *EGFR* mutations is necessary when the patients have some risk factors of acute lung injury by gefitinib treatment (Seto and Yamamoto 2004). Considering high response rate of gefitinib in contrast with high frequency of gefitinib-induced severe lung injury in Japan (AuAstrazeneca 2004, in-house data; Fukuoka et al. 2003), the precise, sensitive methods for detection of *EGFR* mutations are urgently needed especially for Japanese population. Although *EGFR* mutations observed in lung cancer tissues were located between exons 18 and 21, all types do not have equal effects in response to gefitinib (Shigematsu and Gazdar 2006). G719A and A859T were detected in lung cancer patients who experienced progressive diseases after treatment of gefitinib (Han et al. 2005), and T790M was observed at the time of relapse (Kobayashi et al. 2005; Pao et al. 2005). These results indicate that identification of mutation typing is indispensable. A screening system by DHPLC and subsequent direct sequencing for detection of the mutation typing, a quick, sensitive and cost effective method, is useful for not only prediction of gefitinib but also analysis of gefitinib resistance.

## References

- Aoyagi Y, Yokose T, Minami Y, Ochiai A, Iijima T, Morishita Y, Oda T, Fukao K, Noguchi M (2001) Accumulation of losses of heterozygosity and multistep carcinogenesis in pulmonary adenocarcinoma. *Cancer Res* 61:7950–7954
- AuAstrazeneca (2004) In-house data; result and discussion document concerning the prospective investigation on Iressa Tablet 250 (Special investigation)
- “Cancer Statistics in Japan” Editorial Board (2005) Number of deaths and proportional mortality rates from malignant neoplasms by site in Japan. In: Nomura K, Sobue T, Nakatani H, Maehara M, Kiryu Y, Tsukuma H Doi M (eds) *Cancer Statistics in Japan-2005*. Foundation for Promotion Cancer Research, Tokyo, pp 36–39
- Fukuoka M, Yano S, Giaccone G, Tamura T, Nakagawa K, Douillard JY, Nishiwaki Y, Vansteenkiste J, Kudoh S, Rischin D, Eek R, Horai T, Noda K, Takata I, Smit E, Averbuch S, Macleod A, Feyereislova A, Dong RP, Baselga J (2003) Multi-institutional randomized phase II trial of gefitinib for previously treated patients with advanced non-small-cell lung cancer (The IDEAL 1 Trial). *J Clin Oncol* 21:2237–2246
- Han SW, Kim TY, Hwang PG, Jeong S, Kim J, Choi IS, Oh DY, Kim JH, Kim DW, Chung DH, Im SA, Kim YT, Lee JS, Heo DS, Bang YJ, Kim NK (2005) Predictive and prognostic impact of epidermal growth factor receptor mutation in non-small-cell lung cancer patients treated with gefitinib. *J Clin Oncol* 23:2493–2501
- Huang SF, Liu HP, Li LH, Ku YC, Fu YN, Tsai HY, Chen YT, Lin YF, Chang WC, Kuo HP, Wu YC, Chen YR, Tsai SF (2004) High frequency of epidermal growth factor receptor mutations with complex patterns in non-small cell lung cancers related to gefitinib responsiveness in Taiwan. *Clin Cancer Res* 10:8195–8203
- Jorissen RN, Walker F, Pouliot N, Garrett TP, Ward CW, Burgess AW (2003) Epidermal growth factor receptor: mechanisms of activation and signalling. *Exp Cell Res* 284:31–53
- Kim DW, Choy H (2004) Potential role for epidermal growth factor receptor inhibitors in combined-modality therapy for non-small-cell lung cancer. *Int J Radiat Oncol Biol Phys* 59:11–20
- Kobayashi S, Boggon TJ, Dayaram T, Janne PA, Kocher O, Meyerson M, Johnson BE, Eck MJ, Tenen DG, Halmos B (2005) *EGFR* mutation and resistance of non-small-cell lung cancer to gefitinib. *N Engl J Med* 352:786–792
- Kosaka T, Yatabe Y, Endoh H, Kuwano H, Takahashi T, Mitsudomi T (2004) Mutations of the epidermal growth factor receptor gene in lung cancer: biological and clinical implications. *Cancer Res* 64:8919–8923
- Le Calvez F, Mukeria A, Hunt JD, Kelm O, Hung RJ, Taniere P, Brennan P, Boffetta P, Zaridze DG, Hainaut P (2005) TP53 and KRAS mutation load and types in lung cancers in relation to tobacco smoke: distinct patterns in never, former, and current smokers. *Cancer Res* 65:5076–5083
- Lynch TJ, Bell DW, Sordella R, Gurubhagavatula S, Okimoto RA, Brannigan BW, Harris PL, Haserlat SM, Supko JG, Haluska FG, Louis DN, Christiani DC, Settleman J, Haber DA (2004) Activating mutations in the epidermal growth factor receptor underlying responsiveness of non-small-cell lung cancer to gefitinib. *N Engl J Med* 350:2129–2139
- Mountain CF, Dresler CM (1997) Regional lymph node classification for lung cancer staging. *Chest* 111:1718–1723
- Noguchi M, Morikawa A, Kawasaki M, Matsuno Y, Yamada T, Hirohashi S, Kondo H, Shimosato Y (1995) Small

- adenocarcinoma of the lung. Histologic characteristics and prognosis. *Cancer* 75:2844–2852
- Paez JG, Janne PA, Lee JC, Tracy S, Greulich H, Gabriel S, Herman P, Kaye FJ, Lindeman N, Boggon TJ, Naoki K, Sasaki H, Fujii Y, Eck MJ, Sellers WR, Johnson BE, Meyerson M (2004) EGFR mutations in lung cancer: correlation with clinical response to gefitinib therapy. *Science* 304:1497–1500
- Pao W, Miller V, Zakowski M, Doherty J, Politi K, Sarkaria I, Singh B, Heelan R, Rusch V, Fulton L, Mardis E, Kupfer D, Wilson R, Kris M, Varmus H (2004) EGF receptor gene mutations are common in lung cancers from “never smokers” and are associated with sensitivity of tumors to gefitinib and erlotinib. *Proc Natl Acad Sci USA* 101:13306–13311
- Pao W, Miller VA, Politi KA, Riely GJ, Somwar R, Zakowski MF, Kris MG, Varmus H (2005) Acquired resistance of lung adenocarcinomas to gefitinib or erlotinib is associated with a second mutation in the EGFR kinase domain. *PLoS Med* 2:225–235
- Seto T, Yamamoto N (2004) Interstitial lung diseases (ILD) induced by gefitinib in patients with advanced non-small cell lung cancer (NSCLC): results of a West Japan Thoracic Oncology group (WJTOG) epidemiological survey. *Proc Am Soc Clin Oncol* 24:629
- Shigematsu H, Gazdar AF (2006) Somatic mutations of epidermal growth factor receptor signaling pathway in lung cancers. *Int J Cancer* 118:257–262
- Sordella R, Bell DW, Haber DA, Settleman J (2004) Gefitinib-sensitizing EGFR mutations in lung cancer activate anti-apoptotic pathways. *Science* 305:1163–1167
- Tang X, Shigematsu H, Bekele BN, Roth JA, Minna JD, Hong WK, Gazdar AF, Wistuba II (2005) EGFR tyrosine kinase domain mutations are detected in histologically normal respiratory epithelium in lung cancer patients. *Cancer Res* 65:7568–7572
- Tokumo M, Toyooka S, Kiura K, Shigematsu H, Tomii K, Aoe M, Ichimura K, Tsuda T, Yano M, Tsukuda K, Tabata M, Ueoka H, Tanimoto M, Date H, Gazdar AF, Shimizu N (2005) The relationship between epidermal growth factor receptor mutations and clinicopathologic features in non-small cell lung cancers. *Clin Cancer Res* 11:1167–1173
- Westra WH, Baas IO, Hruban RH, Askin FB, Wilson K, Offerhaus GJ, Slebos RJ (1996) K-ras oncogene activation in atypical alveolar hyperplasias of the human lung. *Cancer Res* 56:2224–2228
- Xiao W, Oefner PJ (2001) Denaturing high-performance liquid chromatography: a review. *Hum Mutat* 17:439–474
- Yang SH, Mechanic LE, Yang P, Landi MT, Bowman ED, Wampfler J, Meerzaman D, Hong KM, Mann F, Dracheva T, Fukuoka J, Travis W, Caporaso NE, Harris CC, Jen J (2005) Mutations in the tyrosine kinase domain of the epidermal growth factor receptor in non-small cell lung cancer. *Clin Cancer Res* 11:2106–2110
- Yatabe Y, Kosaka T, Takahashi T, Mitsudomi T (2005) EGFR mutation is specific for terminal respiratory unit type adenocarcinoma. *Am J Surg Pathol* 29:633–639

## Short-Term Culture and $\gamma$ H2AX Flow Cytometry Determine Differences in Individual Radiosensitivity in Human Peripheral T Lymphocytes

Kanya Hamasaki,<sup>1</sup> Kazue Imai,<sup>1</sup> Kei Nakachi,<sup>1</sup> Norio Takahashi,<sup>2</sup> Yoshiaki Kodama,<sup>2</sup> and Yoichiro Kusunoki<sup>1\*</sup>

<sup>1</sup>Department of Radiobiology/Molecular Epidemiology, Radiation Effects Research Foundation, Hiroshima, Japan

<sup>2</sup>Department of Genetics, Radiation Effects Research Foundation, Hiroshima, Japan

Histone H2AX, a subfamily of histone H2A, is phosphorylated and forms proteinaceous repair foci at the sites of DNA double-strand breaks in response to genotoxic insults, such as ionizing radiation. This process is believed to play a key role in the repair of DNA damage. In this study, we established a flow cytometry (FCM) system for measuring radiation-induced phosphorylated histone H2AX ( $\gamma$ H2AX) in cultured human T lymphocytes to evaluate individual radiation sensitivity *in vitro*. Irradiation of short-term (~7 days) cultured T lymphocytes exhibited significant interindividual, but not interexperimental, differences in the cellular content of  $\gamma$ H2AX 6 hr after 4 Gy of X-irradiation in three independent experiments using peripheral blood lymphocytes from six healthy donors. However, these differences were not as

marked in uncultured lymphocytes, or lymphocytes that were cultured for a prolonged period (~13 days). The variation of  $\gamma$ H2AX focus formation in lymphocytes of individuals was reproducible, with differences reaching about 1.5-fold following 7 days of culture. Therefore, the FCM-based  $\gamma$ H2AX measurement appeared to reflect both the temporal course and the amount of DNA damage within the irradiated lymphocytes. Further, we confirmed that the differences in residual lymphocyte subsets were not involved in individual radiosensitivity. These results suggest that the FCM-based  $\gamma$ H2AX assay using cultured T lymphocytes might be useful for the rapid and reliable assessment of individual radiation sensitivity involved in DNA damage repair. *Environ. Mol. Mutagen.* 48:38–47, 2007.

© 2006 Wiley-Liss, Inc.

**Key words:** DNA repair; peripheral blood; radiation effect

### INTRODUCTION

It is believed that interindividual variability in the cellular responses to genotoxic agents, e.g., ionizing radiation, is a critical element in reliably estimating cancer risks in exposed individuals and populations. To assess individual sensitivity to radiation exposure *in vitro*, different endpoints measuring radiation-induced cellular damage, such as DNA strand-breaks, chromosomal damage, and lethality, have been studied. For example, increased radiation sensitivity to chromosome damage has been observed not only in a number of heritable cancer-prone disorders, but also in a significant proportion of sporadic cancer cases [Parshad et al., 1996; Scott et al., 1998, 1999; Roberts et al., 1999; Terzoudi et al., 2000]. A positive association has been demonstrated for humans between chromosome aberration frequency in peripheral blood T lymphocytes and cancer susceptibility [Hagmar et al., 2004]. Further, a possible positive correlation has been recognized between the radiosensitivity of lympho-

cytes irradiated *in vitro* and *in vivo* exposure, specifically when survival is used as the endpoint [West et al., 2001]. Analyses of chromosomal aberrations and estimates of survival responses, which these studies used, are sensitive and reliable biomarkers for the assessment of cellular damage, but they require considerable labor and a high degree of technical skill. Bioindicators of an individual's inherent

Grant sponsors: Ministry of Education, Culture, Sports, Science, and Technology of Japan; The Ministry of Health, Labour and Welfare.

\*Correspondence to: Yoichiro Kusunoki, PhD, Department of Radiobiology/Molecular Epidemiology, Radiation Effects Research Foundation, 5-2 Hijiyama Park, Minami-ku, Hiroshima 732-0815, Japan.  
E-mail: ykusunok@rerf.or.jp

Received 24 August 2006; provisionally accepted 22 September 2006; and in final form 6 October 2006

DOI 10.1002/em.20273

Published online 12 December 2006 in Wiley InterScience (www.interscience.wiley.com).

radiosensitivity, and perhaps cancer risk that is easily and reliably measured, need to be identified and developed, preferably using high throughput assay platforms and highly objective criteria to quantitate endpoints.

It is well known that DNA double-strand breaks (DSBs) in cell nuclei are generated by sufficiently intense exposure to genotoxic agents, including ionizing radiation. In response to DSB generation, histone H2AX, a subfamily of histone H2A, is rapidly phosphorylated by members of the PI3 kinase family (ATM, DNA-PK, and ATR) and forms proteinaceous foci that cover large regions (at least 2 Mb) surrounding DSB sites [Rogakou et al., 1998]. Antibody-specific immunofluorescence has been used to visualize the time course of phosphorylated H2AX ( $\gamma$ H2AX) development and regression in irradiated cell nuclei and indicates that foci continue to grow for about 1 hr after irradiation and then decrease in both size and number as DSB-rejoining proceeds in damaged cells. This process is believed to be critical to cellular repair of DNA damage [Paull et al., 2000; Celeste et al., 2002, 2003; Kobayashi, 2004]. Since the number of  $\gamma$ H2AX foci closely corresponds to the number of DSBs in cells [Rogakou et al., 1999], counting  $\gamma$ H2AX foci has frequently been used to estimate DSBs in cells following genotoxic stress and the subsequent repair of DNA damage. The  $\gamma$ H2AX focus-based assay is generally regarded as being more sensitive in detecting DSBs than more conventional assays, such as pulse-field gel electrophoresis (PFGE), neutral single cell electrophoresis (Comet assay), or the DNA elution assay [Takahashi and Ohnishi, 2005].

Flow cytometry (FCM)-based  $\gamma$ H2AX assays, which have high-speed and high-sensitivity, have been developed previously, but applied solely to assessing the generation and repair of DSBs in various tumor cell lines [MacPhail et al., 2003a,b; Banath et al., 2004]. In this study, we attempted to establish a reliable and straightforward system for detecting *in vitro* radiation-induced DSBs in cultured T lymphocytes from normal healthy humans using  $\gamma$ H2AX FCM. Further, we attempted to validate the assay's applicability for analyzing individual radiation sensitivity in human populations.

## MATERIALS AND METHODS

### Cell Culture

Venous peripheral blood was obtained with informed consent from six healthy adults (four males aged 33, 38, 49, and 49, and two females aged 40 and 49) at our laboratory. We obtained approval from the Human Investigation Committee of the Radiation Effects Research Foundation at the time this study was carried out. Peripheral blood mononuclear cells (PBMCs) were separated by Ficoll-Hypaque density gradient centrifugation (LSM Lymphocyte Separation Medium; MP Biomedicals, Aurora, OH). T-lymphocyte cultures were established and maintained as described previously [Kushiro et al., 1992]. In brief, separated PBMCs were distributed into each well of a 24-well plate (Corning, Corning, NY) at  $5 \times 10^5$  cells/well with 2 ml GIT medium (Wako Pure Chemical

Industry, Osaka, Japan) containing 10% fetal bovine serum (FBS; Inter-gen, New York, NY), 2% L-glutamine (Invitrogen, Carlsbad, CA), 2% penicillin-streptomycin (Invitrogen), 1:3,200 Phytohemagglutinin (PHA; Difco Laboratories, Detroit, MI), and 10 ng/ml human recombinant interleukin-2 (rIL-2; Pepro Tech, London, UK), and cultured for 7 days at 37°C in 5% CO<sub>2</sub> and 95% air. After 7 days of culture, propagated T lymphocytes were collected and resuspended in fresh media for analyses. B-lymphoblastoid cell lines were established by incubating PBMCs with a culture supernatant of Epstein-Barr virus-producing B95-8 cell lines [Kusunoki et al., 1995]. The B-cell lines were maintained by weekly replacement of part of the culture with fresh GIT medium, supplemented with 10% FBS, 2% L-glutamine, and antibiotics.

### X-Irradiation

Cells were resuspended in wells of 24-well plates at an approximate cell concentration of  $1 \times 10^6$  ml, irradiated with 1, 2, 4, or 8 Gy of X-rays, and further cultured for 1, 2, 6, or 24 hr after X-irradiation. Irradiation was performed at a dose rate of 0.7 Gy/min at room temperature using an X-ray irradiator (HF-320; Shimadzu, Kyoto, Japan) equipped with 0.5-mm Al and 0.3-mm Cu filters at 220 kVp and 8 mA. To ensure accurate comparison among different samples, the samples were irradiated simultaneously.

### $\gamma$ H2AX FCM

Cells cultured after X-irradiation were fixed in 70% ethanol at a cell concentration of  $4 \times 10^6$  ml and kept at  $-20^\circ\text{C}$  until use. Fixed cells ( $50 \mu\text{l}$ ,  $2 \times 10^5$ ) were added with 150  $\mu\text{l}$  phosphate buffered saline (PBS; Sigma-Aldrich, St. Louis, MO) in the wells of a 96-well U-bottom plate (Becton Dickinson, Franklin Lakes, NJ) and centrifuged at 450g for 5 min. The cells were washed twice with PBS and then resuspended in 50  $\mu\text{l}$  permeabilization buffer (0.5% saponin, 10 mM HEPES, pH 7.4, 140 mM NaCl, 2.5 mM CaCl<sub>2</sub>). Following incubation with 4  $\mu\text{l}$  mouse monoclonal antiphosphohistone H2A.X (Ser139) antibody (Upstate, Lake Placid, NY) diluted 1:100 with PBS containing 1% FBS, and 0.01% NaN<sub>3</sub> for 20 min at room temperature, the cells were washed with PBS containing 0.1% saponin. Subsequently, 40  $\mu\text{l}$  secondary antibody, Alexa 488 F(ab')<sub>2</sub> fragment of goat antimouse IgG (H + L) (Molecular Probes, Eugene, OR) diluted 1:50 with PBS (containing 1% FBS, 0.01% NaN<sub>3</sub>), was added to the cell pellet, and the cell suspension was incubated for 20 min at room temperature. After the reaction, the cells were washed and resuspended in PBS containing 1% FCS, 0.01% NaN<sub>3</sub> containing 5  $\mu\text{g}/\text{ml}$  propidium iodide (PI; Wako Pure Chemical Industry), and 40 ng/ml RNase A (MP Biomedicals, Aurora, OH) for at least 30 min prior to FCM. Expression levels of  $\gamma$ H2AX in  $1 \times 10^4$  cells were analyzed using a FACScan (BD Biosciences, Franklin Lakes, NJ). Since it was necessary to compare  $\gamma$ H2AX levels within lymphocytes of six healthy adults under the same experimental conditions, all samples were measured on the same day. Data analysis was conducted using Flowjo software (Tree Star, Ashland, OR). Radiation-induced  $\gamma$ H2AX levels were determined by relative  $\gamma$ H2AX fluorescence intensities, i.e., differences between the mean fluorescence of unirradiated and irradiated cells. In a selected number of experiments, appropriate fractions of cultured T lymphocytes were sorted with the cell sorter, JSAN (Bay Bioscience, Kobe, Japan), and subsequently analyzed microscopically. For these cell sorting experiments we used 4' 6-diamidino-2-phenylindole dihydrochloride hydrate (DAPI; Wako Pure Chemical Industries) at 1  $\mu\text{g}/\text{ml}$  instead of PI for DNA staining.

### Lymphocyte Viability and Phenotype

Cultured T cells were stained with FITC-labeled anti-Annexin V (MBL, Nagoya, Japan) and PI, and subsequently assessed for viability using a FCM method described previously [Ohara et al., 2004]. Lymphocyte subsets in both uncultured and cultured cell populations were examined using

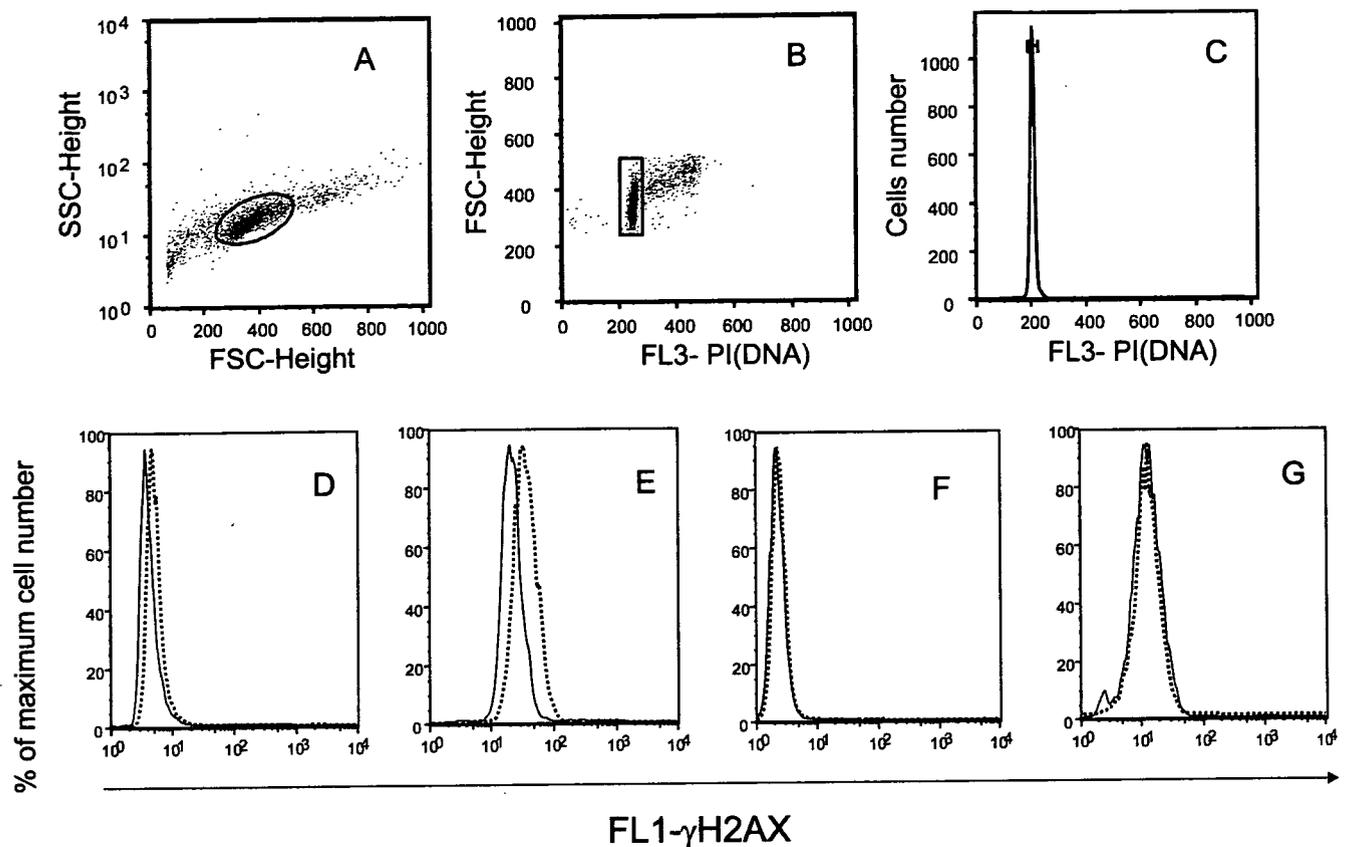


**Fig. 1.** Flow cytometry (FCM) analysis of phosphorylated H2AX ( $\gamma$ H2AX) in cultured T lymphocytes and uncultured lymphocytes 6 hr after 0 or 4 Gy of X-irradiation. Dashed (Donor 2) and solid (Donor 6) lines indicate  $\gamma$ H2AX histograms in two individuals who showed the second highest and the lowest sensitivity to radiation-induced  $\gamma$ H2AX expression among six healthy adults (Fig. 5). (A) Gating on the viable single-cell events based on forward and side light scattering (FSC and

SSC). (B) Subsequent rough gating on the diploid cell fraction. (C) Final strict gating on G1 cells showing the FL3 (PI) peak channel  $\pm 20$  fluorescence units. (D)  $\gamma$ H2AX histograms in the strictly gated G1-cell population of unirradiated cultured T lymphocytes. (E)  $\gamma$ H2AX histograms in 4 Gy irradiated cultured T lymphocytes. (F)  $\gamma$ H2AX histograms in unirradiated fresh lymphocytes. (G)  $\gamma$ H2AX histograms in irradiated fresh lymphocytes.

an FCM method, as described previously [Kusunoki et al., 1998]. For these analyses, cells were stained with CD3-PerCP, CD4-FITC, CD8-PECy5, CD20-PE (BD Biosciences Pharmingen, San Jose, CA), CD16-FITC, or CD45RA-PE antibodies (Beckman Coulter, Miami, FL).

### T-Lymphocyte Sorting

Freshly isolated lymphocytes were stained with PE-labeled CD3, PECy7-labeled CD4, and FITC-labeled antibodies (BD Biosciences). CD3+/CD4+ and CD3+/CD8+ fractions were isolated using JSAN. The cell fractions were then cultured by the method described above, and subsequently used for  $\gamma$ H2AX FCM analyses. The percentages of viable CD3+/CD4+ and CD3+/CD8+ cell fractions recovered after 7 days of culture were 98% and 99%, respectively.

### Fluorescence Microscopy Analysis

Cells stained with anti- $\gamma$ H2AX and Alexa 488-labeled secondary antibodies, as described above, were cyto-centrifuged onto glass slides (Cytospin 3; Shandon, Cheshire, UK), air-dried and mounted with an antifade solution containing 125 ng/ml DAPI.

The cells were visualized with a fluorescence microscope, and representative images were captured and automatically analyzed using Image Pro Plus 4.5 software (Plantron, Tokyo, Japan). The software incorpo-

rated a macroprogram designed to aid in enumerating the number of  $\gamma$ H2AX foci per cell by identifying nucleus position and the associated number of foci via thresholding the area and diameter of foci.

### Statistical Analysis

Distributions of values for  $\gamma$ H2AX levels were analyzed for interindividual or interexperimental variations by one-way analyses of variance (ANOVA). Associations between levels of  $\gamma$ H2AX measured by FCM and the number of  $\gamma$ H2AX foci per cell measured microscopically in appropriate cell fractions were analyzed using the Jonckheere-Terpstra test (SPSS ver. 13.0; SPSS, Chicago, IL).

## RESULTS

### $\gamma$ H2AX FCM Gated on G0/G1 Phase Cells

It is known that  $\gamma$ H2AX focus formation appears not only in cells in which DNA DSBs have been induced, but also in those undergoing DNA synthesis and mitosis [Ichijima et al., 2005; McManus and Hendzel, 2005] or apoptosis [MacPhail et al., 2003b; Mukherjee et al., 2006].

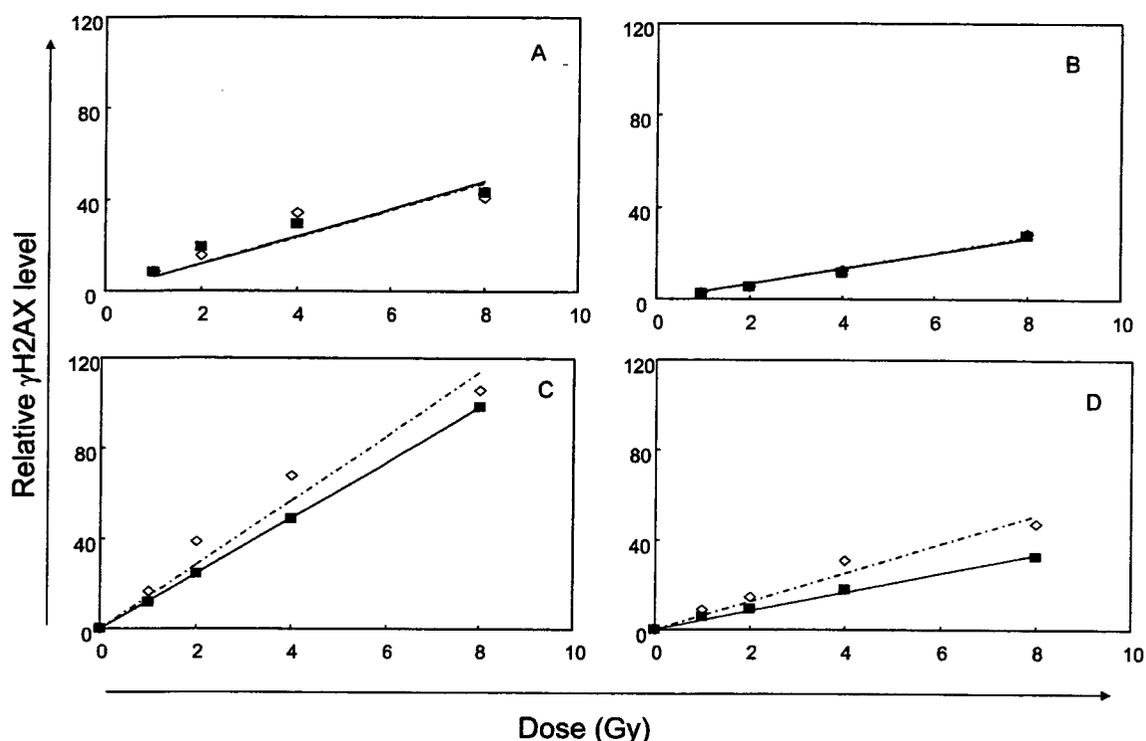


**Fig. 2.** Dose responses of  $\gamma$ H2AX levels in uncultured lymphocytes (A,B) and cultured T lymphocytes (C,D) from Donor 2 (dashed-dotted lines) and Donor 6 (solid lines). Cultured T lymphocytes were irradiated with 0, 1, 2, 4, and 8 Gy of X-rays and analyzed for  $\gamma$ H2AX expression

1 hr (A,C) and 6 hr (B,D) after irradiation. There was a significant linear correlation ( $r > 0.86$ ) between relative  $\gamma$ H2AX level and radiation dose for each donor both 1 and 6 hr after irradiation.

To ensure the accuracy of measurements specific for radiation-induced  $\gamma$ H2AX, X-irradiated cells were simultaneously analyzed for  $\gamma$ H2AX expression and DNA content by FCM. The  $\gamma$ H2AX levels were determined in cell fractions gated on the G0/G1 phase. Figure 1 shows an example of FCM used for determining the  $\gamma$ H2AX level in irradiated cells. After gating on viable single-cell events based on forward and side light scattering (Fig. 1A) and subsequent gating on diploid cells (Fig. 1B), G0/G1 phase cells were clearly distinguished by their DNA content, as reflected by peak channel fluorescence ( $\pm 20$  fluorescence units) from the other events (Fig. 1C). The  $\gamma$ H2AX level in the G0/G1 phase cell populations was determined by the geometric mean of  $\gamma$ H2AX fluorescence.

#### Sensitivity of $\gamma$ H2AX FCM Using Cultured and Uncultured Lymphocyte Populations

Measurements of radiation-induced  $\gamma$ H2AX levels within cultured T lymphocytes and uncultured fresh lymphocytes were carried out and validated using FCM. Figure 1 shows typical FCM patterns observed in cultured and uncultured cells 6 hr after either 0 or 4 Gy of X-irradiation. Donors 2 and 6 provided the cells for these experiments, and as described later, they showed the second highest and the lowest sensitivities to radiation-induced  $\gamma$ H2AX expression

among the six individuals we studied. We detected significant differences in the levels of  $\gamma$ H2AX fluorescence levels between these two individuals in T-lymphocytes cultured for 7 days prior to irradiation, whereas there was no obvious difference in  $\gamma$ H2AX expression level when we used uncultured lymphocytes (Fig. 2). A linear relationship existed between radiation dose and  $\gamma$ H2AX expression level in both cultured and uncultured lymphocytes from both of these individuals (Fig. 2). One hour after irradiation, the radiation dose effect in uncultured lymphocytes was about half of that found in cultured T lymphocytes (Fig. 2A). Six hours after irradiation, a similar difference also was observed between uncultured and cultured lymphocytes for Donor 2, whereas the dose effect difference was smaller for Donor 6 (Fig. 2C). We also observed by FCM a clear difference in the dose response of  $\gamma$ H2AX expression by cultured T lymphocytes of these two individuals when assayed at 1 and 6 hr after irradiation. By contrast, the difference in the dose response was not obvious in uncultured lymphocytes from the same donors.

Although we also tested EBV-transformed B-cell lines for  $\gamma$ H2AX expression after irradiation, and obtained similar dose responses to those of cultured T lymphocytes, the responses of several B-cell lines prepared from the same six blood donors were not as consistent in terms of the  $\gamma$ H2AX levels produced by given doses of irradiation (data not shown). These results suggest that in terms of



analyzing individual variability in the level of radiation-induced  $\gamma$ H2AX expression by FCM, cultured T lymphocytes are preferable to the other sources, in terms of sensitivity and reliability.

**Preirradiation Cultures and Postirradiation Time Course**

Changes of  $\gamma$ H2AX levels in cultured T lymphocytes from the six healthy adults were analyzed at 1, 2, 6, and 24 hr after 4 Gy irradiation in three independent experiments. Results from a typical experiment are shown in Figure 3. The  $\gamma$ H2AX level reached a peak 1 or 2 hr after radiation exposure and then gradually decreased with

time. Even though the time-course pattern did not differ appreciably among the individuals, variations in  $\gamma$ H2AX levels were observed at various times following irradiation. For example,  $\gamma$ H2AX levels, 6 hr after 4 Gy irradiation, differed by about 1.5-fold in the highest vs. the lowest responding donors. Next, we examined whether the period of T-cell culture before irradiation affected the reliability of  $\gamma$ H2AX measurement for individual variability. For this experiment, cells from the two individuals who showed the second highest and the lowest  $\gamma$ H2AX levels at 6 hr after irradiation were used (i.e., as does the experiment shown in Figure 3; Donors 2 and 6). As shown in Figure 4, similar differences between these two individuals were detected when T lymphocytes were cultured for 5–13 days before irradiation. However, the difference was not as obvious in T lymphocytes cultured for 13 days as in those cultured for 5–10 days (Fig. 4).

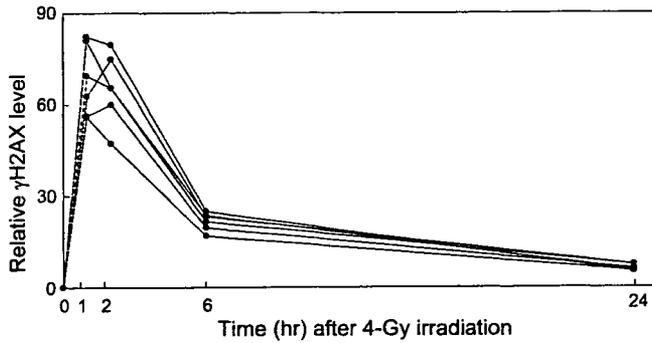


**Fig. 3.** Time course of radiation-induced  $\gamma$ H2AX expression in cultured T lymphocytes from six healthy individuals. Cellular  $\gamma$ H2AX levels were measured 1, 2, 6, and 24 hr after 4 Gy irradiation. The vertical axis indicates relative  $\gamma$ H2AX fluorescence intensity, which is the geometrical mean of the  $\gamma$ H2AX level in irradiated cells minus that in unirradiated cells.

**Interindividual and Interexperimental Variations in  $\gamma$ H2AX Level**

To assess whether individual differences in radiation-induced  $\gamma$ H2AX levels could be observed reproducibly, three independent experiments were carried out using T lymphocytes obtained at different times from the same six individuals. Lymphocytes were cultured for 7 days before 4 Gy irradiation, and both interindividual and interexperimental variations were analyzed statistically for each time point after irradiation. Interindividual variation in radiation-induced  $\gamma$ H2AX levels was highly significant for every time point (Fig. 5). Although interexperimental varia-

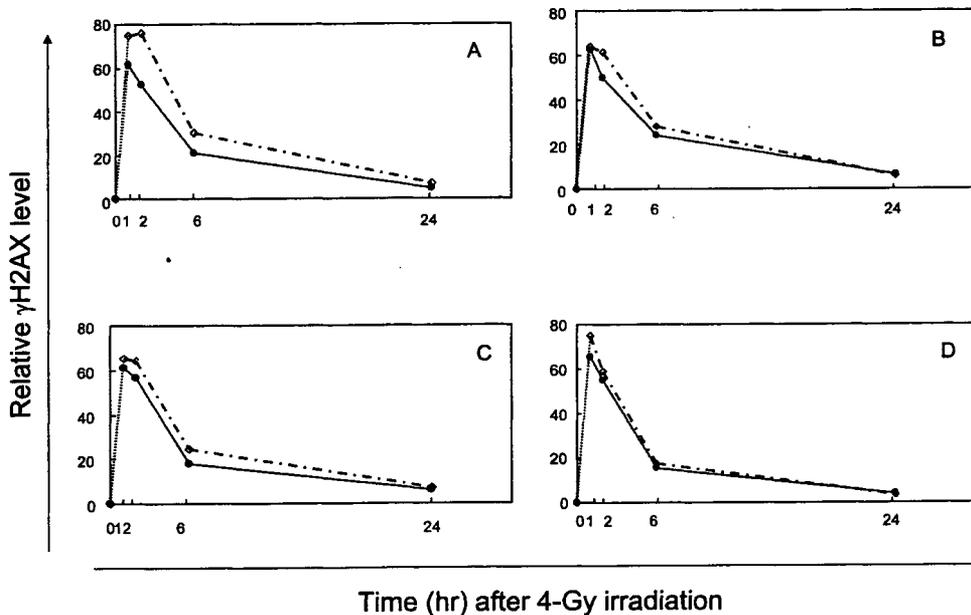


**Fig. 4.** Time course of levels of radiation-induced  $\gamma$ H2AX expression in T lymphocytes cultured for 5 (A), 7 (B), 10 (C), and 13 (D) days from Donors 2 (dashed-dotted lines) and 6 (solid lines).  $\gamma$ H2AX levels

were measured 1, 2, 6, and 24 hr after 4 Gy irradiation. The vertical axis indicates relative  $\gamma$ H2AX intensity, which is the geometrical mean of the  $\gamma$ H2AX level in irradiated cells minus that in unirradiated cells.

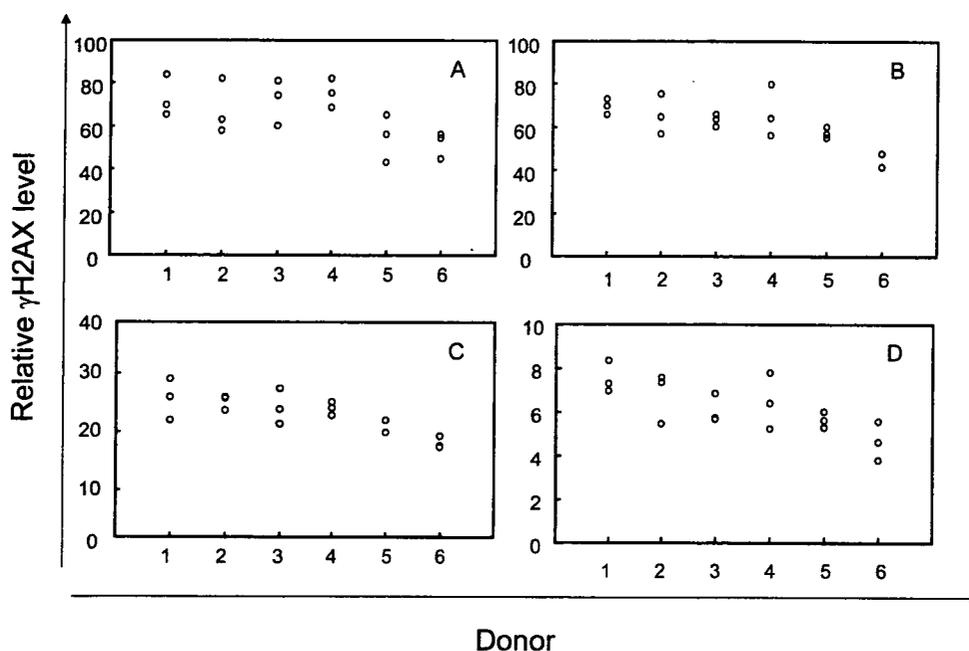


**Fig. 5.** Variability in the level of radiation-induced  $\gamma$ H2AX among six healthy adults. Three independent experiments were carried out using T lymphocytes obtained from the same six individuals and cultured for 7 days before 4 Gy irradiation. Values obtained from the same experiment are plotted with the same symbols. Distributions of individual values for radiation-induced  $\gamma$ H2AX level were analyzed for interindividual and interexperimental variation by one-way analysis of variance (ANOVA). (A) Relative  $\gamma$ H2AX levels 1 hr after irradiation. Interindividual variability:

$F = 8.46$ ;  $P = 0.002$ . Interexperimental variability:  $F = 11.5$ ;  $P = 0.003$ . (B) The levels, 2 hr after irradiation. Interindividual variability:  $F = 7.99$ ;  $P = 0.003$ . Interexperimental variability:  $F = 3.13$ ;  $P = 0.088$ . (C) The levels 6 hr after irradiation. Interindividual variability:  $F = 6.23$ ;  $P = 0.007$ . Interexperimental variability:  $F = 1.64$ ;  $P = 0.243$ . (D) The levels 24 hr after irradiation. Interindividual variability:  $F = 5.25$ ;  $P = 0.013$ . Interexperimental variability:  $F = 3.64$ ;  $P = 0.065$ .

tion was significant, or marginally so, for 1 and 2 hr after irradiation, there was no significant interexperimental variation in the  $\gamma$ H2AX level 6 hr after irradiation. These results suggest that for the assessment of individual radiation sensitivity relative to radiation-induced  $\gamma$ H2AX levels, measurements tested at 6 hr after irradiation are the most reliable.

#### Relationship Between $\gamma$ H2AX Level Measured by FCM and Number of $\gamma$ H2AX Foci Visualized by Microscopy

To ensure that the  $\gamma$ H2AX level determined by FCM corresponded to the number of  $\gamma$ H2AX foci in each cell, we sorted and collected three appropriate fractions showing different levels of  $\gamma$ H2AX and counted by fluorescence microscopy the number of  $\gamma$ H2AX foci per cell in each of the fractions collected. As shown in Figure 6, the level of  $\gamma$ H2AX measured by FCM almost paralleled the mean number of  $\gamma$ H2AX foci per cell in each fraction. Statistical analysis using the Jonckheere-Terpstra test indicated that there was a significant association between the values determined by these different assays ( $P < 0.001$ ).

We also analyzed the number of  $\gamma$ H2AX foci in irradiated cells of individuals with high and low T-cell radiosensitivity (Donors 2 and 6) and found that the  $\gamma$ H2AX levels analyzed by FCM closely corresponded with the

number of  $\gamma$ H2AX foci observed microscopically (Fig. 7). Because the number of  $\gamma$ H2AX foci represents the number of DSBs in irradiated cells [Rogakou et al., 1999] and positively correlates with radiosensitivity of the cells [MacPhail et al., 2003a], differences in the level of  $\gamma$ H2AX expression 6 hr after irradiation may reflect the difference in unrepaired DSBs. It should be noted, however, that there was no indication of radiation-induced apoptosis in cultured T lymphocytes within this 6 hr postirradiation time-frame (data not shown). This suggests that the radiation-induced  $\gamma$ H2AX expression detected in the present study by either FCM or by microscopy probably does not involve apoptosis-related events resulting from radiation exposure.

#### Lymphocyte Subsets and Radiation-Induced $\gamma$ H2AX Levels

To characterize more fully the lymphocyte pools used in the FCM- $\gamma$ H2AX assays, we determined the percentages of lymphocyte subsets (CD3, CD4, CD8, CD16, and CD20) before and 7 days after culture for the six individuals we studied. The cell population just before irradiation was mainly composed of CD4 (10–40%) and CD8 (60–80%) T-cell populations, and a majority of these T-cell populations expressed a low level of CD45RA, a memory-phenotype indication. Other lymphocyte populations,

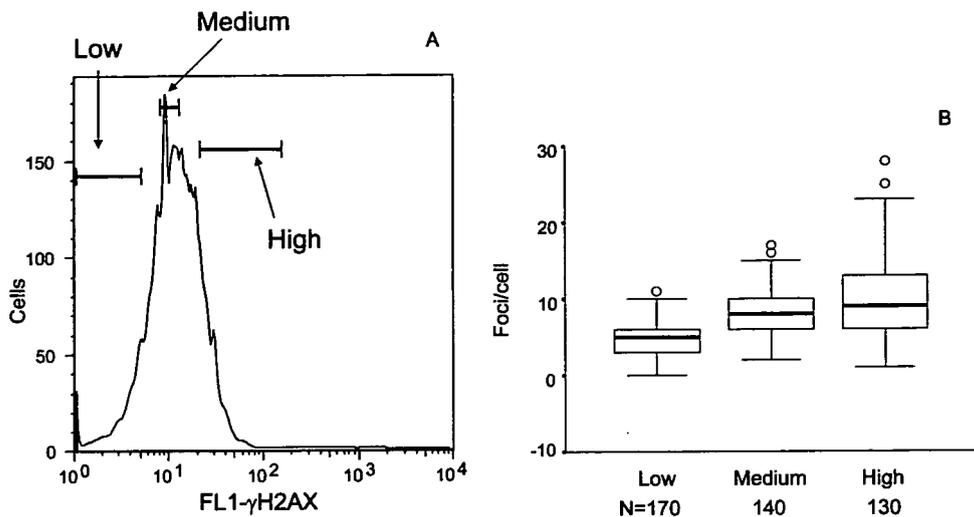
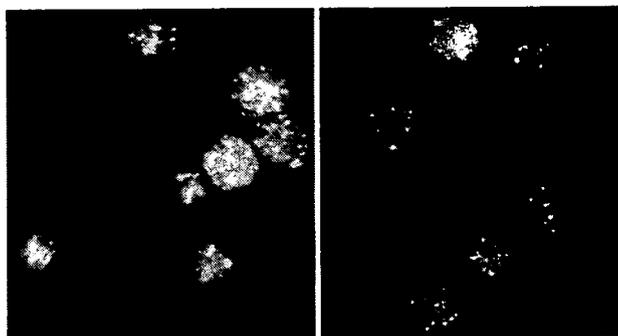


**Fig. 6.** Associations between  $\gamma$ H2AX levels measured with FCM and the number of  $\gamma$ H2AX foci determined by fluorescence microscopy in irradiated cultured T-lymphocyte fractions from one individual (Donor 2). (A) Each cell fraction showing low (1–5 fluorescence channels), medium (8–13 fluorescence channels), or high (21–160 fluorescence channels)  $\gamma$ H2AX fluorescence intensities was sorted from cultured T lymphocytes obtained from one individual and stained for  $\gamma$ H2AX expression 6 hr after 2 Gy irradiation. (B) Box plots of the number of foci per cell in each cell fraction. Totally 130–170 cells for each fraction were analyzed by fluorescence microscopy using Image Pro Plus 4.5 software. The horizontal line in each of the middle of boxes marks the median

value in each fraction. The lower and upper edges of each box mark the 25th and 75th percentiles, respectively, and thus the central 50% of the data values fall within the range of the box. The vertical lines extending up and down from each box show the largest and the smallest values observed, respectively, and open circles mark the “outside values,” which are between 1.5- and 3.0-times higher than the 75th percentile values. The Jonckheere-Terpstra test indicated that there was a significant association between  $\gamma$ H2AX levels measured with FCM and the number of  $\gamma$ H2AX foci determined by fluorescence microscopy ( $P < 0.001$ ).



	Donor 2	Donor 6
Number of foci	1085	1082
Cells analyzed	117	147
Average (foci / cell) $\pm$ SD	9.3 $\pm$ 5.6	7.4 $\pm$ 4.9

$p < 0.004$

**Fig. 7.** Fluorescence microscopy analysis of  $\gamma$ H2AX foci in cultured T lymphocytes from two individuals (Donors 2 and 6). The number of foci in cells was analyzed 6 hr after 4 Gy irradiation using Image Pro Plus

4.5 software. The average number of  $\gamma$ H2AX foci per cell differed significantly between these two individuals ( $P = 0.004$ , the Students' *t*-test).

namely B and NK cells, were quite small (less than 3%). There was no obvious relationship between levels of radiation-induced  $\gamma$ H2AX in individuals and percentages of lymphocyte subsets either before or after cell culture (data not shown). To further support the idea that differences in the CD4 and CD8 T-cell ratio does not contribute to individual differences in radiation-induced  $\gamma$ H2AX

expression, we analyzed  $\gamma$ H2AX levels in separately cultured and irradiated CD4 and CD8 T-cell fractions from Donors 2 and 6. There was no obvious difference in the levels of radiation-induced  $\gamma$ H2AX between CD4 and CD8 T-cell subsets in the same individuals. Difference between these individuals in terms of these subsets were apparent, i.e.,  $\gamma$ H2AX levels in CD4 and CD8 T-cell sub-

sets of Donor 2, 6 hr after 4 Gy irradiation were 32.0 and 28.7, respectively, whereas those in the comparable subsets of Donor 6 were 26.4 and 24.3, respectively. These results suggest that the differences in radiation-induced  $\gamma$ H2AX levels in cultured T lymphocytes between individuals are not related to differences in the proportion of lymphocyte subsets within the test samples.

## DISCUSSION

In this study, we established an FCM system for measuring levels of radiation-induced  $\gamma$ H2AX in human lymphocytes to assess individual differences in radiation sensitivity to DNA damage *in vitro*. Currently,  $\gamma$ H2AX focus formation is being used as a DNA damage marker, specifically for DSBs induced by exposure to various genotoxic agents, such as ionizing radiation [Rogakou et al., 1999].  $\gamma$ H2AX recruits other enzymes related to the DNA repair process (such as 53BP1, BRCA1, the NBS/MRE11/RAD50 complex), and thereby plays a key role in early phases of the repair of damaged cells [Paull et al., 2000; Celeste et al., 2002, 2003; Kobayashi, 2004]. We thought that by measuring cellular levels of  $\gamma$ H2AX by high-throughput FCM, a rapid and accurate assessment of radiation sensitivity in human individuals might be possible. It has been reported that the background  $\gamma$ H2AX level in normal cells differs at each phase of the cell cycle and appears particularly high at the S to G2/M phases [Ichijima et al., 2005; McManus and Hendzel, 2005]. Our FCM system can analyze radiation-induced  $\gamma$ H2AX levels in cells at each phase of the cell cycle, which has been very difficult using conventional fluorescence microscopy analysis. Therefore, one major advantage of our method is that G1-phase cells, with low background  $\gamma$ H2AX levels, can be selectively targeted for analyses.

We expect that the  $\gamma$ H2AX FCM system established in this study will allow straightforward assessments of both individual sensitivity to radiation-induced DNA damage and individual ability to repair such DNA damage. By applying  $\gamma$ H2AX FCM to an epidemiological follow-up study cohort, such as the A-bomb survivor populations in Hiroshima and Nagasaki, we will be able to address the important question of whether or not individuals who have lower DNA repair ability have higher mutability in response to radiation, and in turn, higher risks of radiation-related cancers.

In this study, radiation-induced  $\gamma$ H2AX levels in blood lymphocytes appeared to be about 1.5-fold higher if the cells were cultured for 7 days prior to radiation exposure (Fig. 2). It is highly likely that growth-stimulated T lymphocytes (via PHA and IL-2) were more severely damaged by ionizing radiation than were resting peripheral blood lymphocytes. This is consistent with an earlier find-

ing of 20-fold increases in DNA repair synthesis following ionizing irradiation of stimulated lymphocytes compared with resting lymphocytes [Lavin and Kidson, 1977]. However, it is unclear why individual differences in radiation-induced  $\gamma$ H2AX levels can be detected more readily in cultured T lymphocytes than in freshly isolated and resting lymphocytes. This partly may be due to the relatively low  $\gamma$ H2AX levels within resting irradiated lymphocytes that have not been growth-activated *in vitro* and the substantial differences in metabolic status between cultured and uncultured lymphocytes, such as specific variations in activities of DNA repair enzymes. However, it has been previously reported that the transcriptional levels of most DNA repair genes were not significantly increased in PHA-stimulated lymphocytes when compared with levels in resting lymphocytes [Mayer et al., 2002]. Therefore, it is unlikely that differences in the activity of DNA repair genes are the cause of individual differences in residual  $\gamma$ H2AX levels in irradiated cultured T lymphocytes. Alternatively, differences in radiation sensitivity between cultured and uncultured T lymphocytes might result from differences in the ability of irradiated cells to scavenge DNA-damaging radicals induced by ionizing radiation. Further testing is required regarding whether the genes responsible for radical scavenger proteins are substantially upregulated in cultured T lymphocytes, and whether there are differences in levels of these proteins in cultured T lymphocytes from different individuals.

Differences in individual radiosensitivity were not as obvious in T lymphocytes cultured for 13 days (Fig. 4). Previously, it had been shown that the cell growth rate declined appreciably in similar T-cell cultures 10–14 days after the beginning of culture [Ishioka et al., 1997]. This decline may have been simply due to growth arrest mediated by attenuated T-cell receptor and/or growth factor signals. Simply stated, the diminished responses were probably the result of the cultured T lymphocytes being in a resting state at the time of testing (13th day).

$\gamma$ H2AX levels detected with FCM in a given fraction of irradiated T lymphocytes were able to fully reflect the mean number of microscopically detected  $\gamma$ H2AX foci per cell in the same fraction (Fig. 6). It is probable that the  $\gamma$ H2AX detected by FCM was related to the levels of radiation-induced DSBs in the same fraction as well. It is therefore likely that individual differences observed in  $\gamma$ H2AX-FCM are related to differences in the degree of DNA damage and in the individual's ability to repair DNA damage.

In this study, there was no obvious difference in radiation-induced  $\gamma$ H2AX levels between CD4 and CD8 T-cell populations obtained and cultured from the same individuals. Our previous study [Nakamura et al., 1990] showed that survival fractions after *in vitro* irradiation did not differ significantly between these subsets when they were isolated from the same individuals and irradiated before